Available online at www.sciencedirect.com
SCIENCE DIRECT
ELSEVIER
International Journal of Solids and Structures 43 (2006) 1372–1387
INTERNATIONAL JOURNAL OF SOLIDS and STRUCTURES
www.elsevier.com/locate/ijsolstr

Experimental study and analysis of RC beams strengthened with CFRP laminates under sustaining load

Wang Wenwei [a,*], Li Guo [b]

[a] Department of Bridge Engineering of Transportation College, Southeast University, Nanjing 210096, PR China
[b] Department of Civil Engineering, Dalian University of Technology, Dalian 116023, PR China

Received 28 July 2004; received in revised form 22 March 2005

Abstract

Six reinforced concrete beams strengthened in flexure using carbon fiber reinforced polymer (CFRP) laminates subjected to different sustaining loads were tested. The main goal of the test is to examine the effects of initial load and load history on the ultimate strength of strengthened reinforced concrete beams by externally bonded CFRP laminates. The main experimental parameters include different levels of sustaining load at the time of strengthening and load history. To explain the experimental results in quantitative terms, a theoretical model for flexural behavior of the strengthened reinforced concrete beam is also developed. Test results in the current study show that sustaining load levels at the time of strengthening have important influence on the ultimate strength of strengthened reinforced concrete beams. If the initial load is basically same, the ultimate strength of reinforced concrete beams strengthened with CFRP laminates is almost same regardless of load history at the time of strengthening.

Keywords: Experimental study; RC beams; Strengthening; CFRP; Sustaining load; Load history

1. Introduction

The repair of structurally deteriorated reinforced concrete structures becomes necessary as the structural element ceases to provide satisfactory over loading, strength, and serviceability. In recent years, the development of fiber reinforced polymer (FRP) material, with a high-strength-to-weight ratio and excellent resistance to electrochemical corrosion (see for references Erki and Rizkalla, 1993; Charles, 1999; Sami and Pieere, 1999), makes it particularly suited to structural applications. Field application of repair by

* Corresponding author. Tel.: +86 25 83794100; fax: +86 25 83792297.
E-mail address: wang_wenwei@sina.com (W. Wenwei).

0020-7683/$ - see front matter © 2005 Elsevier Ltd. All rights reserved.
doi:10.1016/j.ijsolstr.2005.03.076

epoxy-bonded FRP laminates is now recognized to be an effective and convenient method because of the good performance of FRP.

In the literature, there are numerous articles reporting the behavior of virgin beams reinforced externally with FRP for the purpose of increasing the load-carrying capacity (see for references Jones et al., 1980; Saadatmanesh and Ehsani, 1991; Chajes et al., 1994; Arduini et al., 1997; Norris et al., 1997). The reported studies have shown that externally bonded FRP can be effectively used to increase the strength and stiffness of reinforced concrete (RC) beams while maintaining an adequate level of deformability. Several organizations, including ACI Committee 440, ISIS-Canada, and CFRRA-Japan, are developing extensive design guidelines for the use of carbon fiber reinforced polymer (CFRP), indicating that the process of standardization is underway (see for reference Thomas (2003)).

In contrast to the case for member strengthening, several experimental studies have focused on the use of CFRP sheet for the repair of load-damaged RC beams (see for references Arduini and Nanni, 1997; Bonacci and Maalej, 2000; Shahawy et al., 2001; Yeong-soo and Chadon, 2003). This paper presents the results of experimental studies concerning the flexural strengthen of RC beams by the externally bonding of CFRP laminates to the tension face of the beams under different levels of sustaining load, which is an important practical aspect to be considered in standardized repair techniques. At the same time, a calculation method is proposed to investigate the ultimate load capacity.

2. Summary of related studies

The present work is geared toward evaluating the use of CFRP laminates to repair load-damaged RC beams—a practical application that has received little attention in experimental research. In this regard, it is important to distinguish controlled experimental research.

One recently published article (e.g. Yeong-soo and Chadon, 2003) focused on the effect of sustaining load on the flexural behavior of repaired RC beams. Yeong-soo and Chadon (2003) tested six beams strengthened with CFRP laminates subjected to different sustaining loads. The levels of sustaining load at the time of strengthening corresponded to 0%, 50% and 70% of nominal flexural strength of nonstrengthened RC beam, respectively. Results of experiment showed that sustaining load levels at the time of strengthening had more influence on deflections of beams at the yielding and at ultimate stage than the ultimate strength of the beam. In the test, all strengthened beams failed by ripoff rather than tensile rupture of CFRP laminates; hence, it was difficult to judge the effect of strengthening at different levels of sustaining load on the ultimate strength of those beams.

Shahawy et al. (2001) conducted a study on eight full-scale 20 ft long RC T-girders. A control girder with no wrap and a reference girder with two layers of CFRP wrap were tested up to failure in one run for comparison purposes. The girders were preload up to 65%, 85% and 117% of control yield moment and locked and strengthened with two layers of CFRP wrap before resuming the loading up to failure. The results demonstrated the effectiveness of the externally bonded CFRP in repairing load-induced damage in the RC beams. The level of preload prior to installation of CFRP did not affect the overall behavior of the wrapped specimens.

Bonacci and Maalej (2000) tested one beam, which named B3, to study the effect of sustaining load on the performance of member reinforced with CFRP. In John's test, three cycles of load between 45 kN and 90 kN were applied, after which the load was held constant at 45 kN for a period of 1 week to allow application CFRP. CFRP debonding failure mode was observed. The test results show that two layers of CFRP external reinforcement gave beam B3 strength gains of 28% over the control beam B2, which was strengthened with two layers of CFRP at zero load.

Arduini and Nanni (1997) studied the behavior of precracked beams strengthened with CFRP sheets. Their experimental program included short-and medium-length RC beams that were preloaded and

cracked prior to the application of the FRP. Only two specimens were maintained load during the application and curing of the FRP. The results showed that specimens that were precracked showed lower ultimate capacity and stiffness than their virgin counterparts. For damaged specimens, a specimen repaired without sustaining load had an average strength increase of 24% (over the control), while a specimen repaired under sustaining vertical load had a strength increase of only 16% (over the control). Because failure was controlled debonding of the FRP, there was not a substantial difference in ultimate capacity of the specimens.

In this work, the use of CFRP laminates to strengthen preloaded RC beams under different levels of sustaining load was investigated. Six RC beams were loaded to a predetermined level of the ultimate capacity of control beam and locked and strengthened by CFRP laminates.

3. Experimental program

3.1. Test beams details

A total of seven beams were tested. All beams have identical rectangular cross-sections and the same size: 150 mm × 250 mm × 2700 mm. All beams were tested in four-point bending over a simple span (Fig. 1). Variables in the test plan included different levels of sustaining load at the time of strengthening and load history. One beam was used as control specimen and the other six beams were strengthened in flexure using two layers of externally bonded CFRP laminates under different levels of sustaining load. The test specimens are summarized in Table 1. The main flexural reinforcement consisted of three 14 mm deformed bars with a sectional area of 462 mm^2 and steel ratios 1.43% was used (Fig. 1). Two 8 mm round bars with a sectional area of 100.5 mm^2 were used as compression reinforcement (Fig. 1). Shear reinforcement consisted

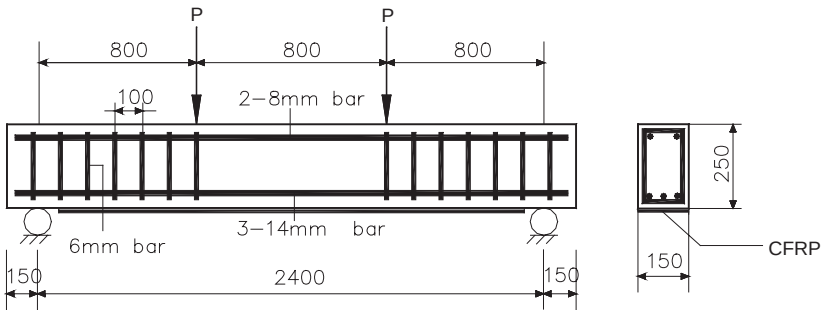

Fig. 1. Details of test beams (dimensions in mm).

Table 1
Test specimen

Beam designation	Repair scheme	CFRP	Load history
CL30	None	None	None
CFC30	2 layers	2300 × 150 × 0.222	Virgin
DBL30-1	2 layers	2300 × 150 × 0.222	0 → 25 kN → sustaining loading → bonding CFRP → failure
DBL30-2	2 layers	2300 × 150 × 0.222	0 → 70 kN → sustaining loading → bonding CFRP → failure
RDBL30-1A	2 layers	2300 × 150 × 0.222	0 → 70 kN → 25 kN → sustaining loading → bonding CFRP → failure
DBL30-3	2 layers	2300 × 150 × 0.222	0 → 90 kN → sustaining loading → bonding CFRP → failure
RDBL30-1B	2 layers	2300 × 150 × 0.222	0 → 90 kN → 25 kN → sustaining loading → bonding CFRP → failure

of 6 mm-diameter round steel stirrups spaced at 100 mm center–center (Fig. 1). The beams were reinforced in this manner to prevent shear failure and to isolate the flexural behavior from shear behavior.

3.2. Material properties

Concrete was designed with grade of compressive strength of C30 according to Chinese Standard *Code for Design of Concrete Structures GB50010-2000* (see reference China Ministry of Construction (2002)). Twenty 150 mm × 150 mm × 150 mm concrete cube specimens were made at the time of casting and were kept with the beams during curing. The average 28-day concrete cube strength f_c was 40.3 MPa. The notation f_c denotes concrete cube strength. The relationship of cylinder strength and cube strength is $f'_c = 0.79 - 0.81 f_c$. The measured yield strength of the 8 mm round rebar was 352.1 MPa and 14 mm deformed rebar was 365.9 MPa. The CFRP material was consisted of 150 mm wide and 0.111 mm thick carbon laminates externally bonded to the tension face of the concrete beams using a two-part epoxy mixed at 2.5:1 ratio and cured at room temperature. Tensile strength, modulus, and elongation of the CFRP material were 3350 MPa, 212 GPa, and 1.58%, respectively. A summary of all the material properties is given in Table 2.

3.3. Testing procedure

For each beam, each longitudinal steel bar was instrumented with one electrical resistance strain gauge at midspan. In addition, each test beam with CFRP laminates was instrumented with two strain gauges at midspan. A total of three linear voltage displacement transducers (LVDTs) were used to measure midspan, and supporting points deflection.

All specimens were tested in four-point bending over a 2.4 m simple span in a 5000-kN test frame. Loads are applied by screw jack fixed to the strong frame throughout the test procedure. The screw jack is devised with safety-holding nuts to maintain the desired levels of sustaining load. The two load points were offset 400 mm from the midspan of the beam, as illustrated in Fig. 2. To define the preloading condition of the damaged beams, one control beam was tested to failure for evaluating cracking, yielding, and ultimate loads. The cracking, yielding, and ultimate loads of the control beam were 28 kN, 85 kN, and 102 kN, respectively. The other six beams were preloaded to expectable loads (Table 1), after which the load was held constant at expectable loads for a period of 1 week to allow for application and curing of the CFRP laminates.

When the preload reaches the desired levels of sustaining load, safety-holding nuts are locked and strengthening work is performed by bonding CFRP laminates to the beam soffits. The procedures of applying CFRP laminates to concrete involved surface preparation, priming, resin undercoating, carbon fiber laminates applying, and resin undercoating. The bottom concrete surface was prepared by polishing until the fine aggregates were exposed and cleaned with acetone. After that, a two-part primer was applied to the prepared concrete surface and left to dry. Next, a two-part epoxy resin was applied to the primed concrete

Table 2
Material properties

Material		f_y (MPa)	ε_y (%)	f_u (MPa)	ε_u (%)	E (GPa)
Steel	8 mmbar	352.1	1.68	523.9		210
	14 mmbar	365.9	1.83	535.9		200
Concrete	C30			40.3		32.7
CFRP				3350	1.58	212

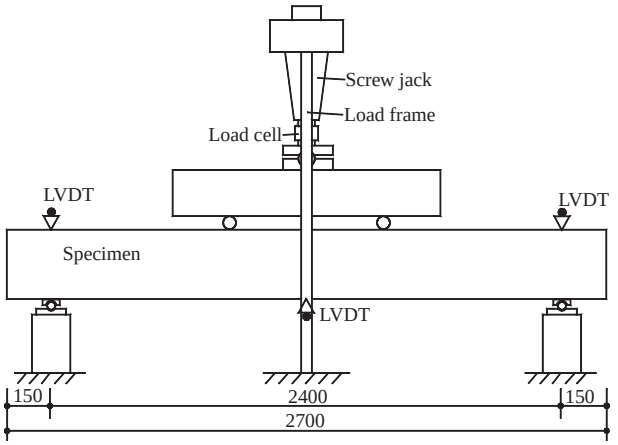

Fig. 2. Test setup.

surface, followed by application of the CFRP laminates. Finally, a resin over coating was applied over the CFRP laminates.

4. Results and discussion

4.1. Load–deflection curves and failure modes

Load–deflection responses for the beams are shown in Figs. 5 and 6 and are summarized in Table 3. For all strengthened beam, there was an increase in the load-carrying capacity when CFRP external reinforcement was added. The increase ranged between 25.5% and 41.2% of the load-carrying capacity of control beam (CL30). The test beams exhibited three failure modes. For the control beam (CL30), failure (Mode I) was by crushing of the concrete in the compression zone after tension steel yield. For the beams (DBL30-1, DBL30-2, RDBL30-1A and RDBL30-1B), failure (Mode II) occurred by the rupture of CFRP accompanied by horizontal cracking in the tension zone in the vicinity of the tension steel, as illustrated in Fig. 3. For the beam (DBL30-3), shear compression failure (Mode III) occurred by crushing of the concrete in the shear compression zone, as illustrated in Fig. 4.

Fig. 5 shows load–deflection curves of nonstrengthened control beam CL30, initially strengthened beam CFC30, and strengthened beams DBL30-1, DBL30-2, and DBL30-3. It could be observed that there are no discernible differences in the stiffness before the longitudinal steel yielding, as shown in Fig. 5. Load–deflection curves show that the stiffness of beams DBL30-1, DBL30-2 and DBL30-2 is weaker than that of CFC30 and stronger than that of CL30 after the longitudinal yielding.

Beam DBL30-1 was strengthened with two longitudinal layers of CFRP laminates under a 25 kN sustaining load. The beam was not cracked after the desired sustaining load was applied. After strengthening, as the additional load applied, flexural cracks were initiated from the bottom of beams in the region of maximum moment. When the load beyond the yield strength of strengthened beam was applied, these cracks were widened and extended upward and new flexural cracks formed. As the applied load was further increased, cracks propagated toward the upper of beam and failure of tensile of CFRP laminates occurred.

Beam DBL30-2 was strengthened with two longitudinal layers of CFRP laminates under a 70 kN sustaining load. A few cracks had formed as the sustaining load applied. After strengthening, the cracks that had been developed up to the sustaining load level continuously propagated upward and a number

Table 3
Experimental and analytical results for loads and deflection

Beam designation	Experimental results				Analytical results			Ductility index = $\frac{\text{Col.(5)}}{\text{Col.(3)}}$	% of control	Modes of failure
	At yield		At failure		$\text{Load}_{\text{yield}}$ (kN)	$\text{Load}_{\text{fail}}$ (kN)	M [a]			
	Load (kN)	Deflection (mm)	Load (kN)	Deflection (mm)						
(1)	(2)	(3)	(4)	(5)	(6)	(7)	(8)	(9)	(10)	(11)
CL30	85	10.02	102	33.4	79.5	83.9		3.33		Concrete crushing
CFC30	90	9.86	140	21.93	88.3	134.3	117.4	2.22	37.3	CFRP rupture
DBL30-1	90	10.96	135	31.94	86.8	133.3	115.7	2.91	32.4	CFRP rupture
DBL30-2	90	10.46	125	29.6	81.5	129.7	112.7	2.82	22.5	CFRP rupture
RDBL30-1A	90	10.2	125	23.31	86.8	133.3	115.7	2.29	22.5	CFRP rupture
DBL30-3	100	10.84	145	30.62	79.0	128.1	111.4	2.82	41.2	Concrete shear compression failure
RDBL30-1B	100	11.27	128	23.32	86.8	133.3	115.7	2.07	25.5	CFRP rupture

[a] M = Mahmoud's model.

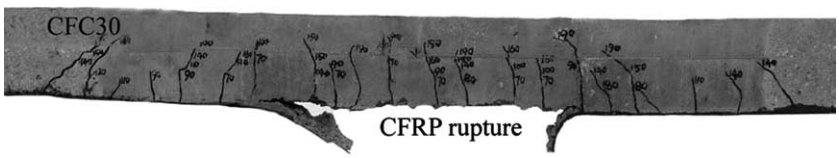

Fig. 3. Mode II failure: rupture of CFRP.

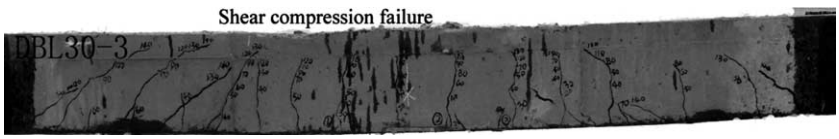

Fig. 4. Mode III failure: crushing of the concrete in the shear compression zone.

of additional cracks between these exiting cracks were formed as the additional load was applied beyond 70 kN. By comparison with beam DBL30-1, similar behavior and failure mode were also observed when the load beyond the yield strength of strengthened beam was applied.

Beam DBL30-3 was strengthened with two longitudinal layers of CFRP laminates under a 90 kN sustaining load. It is remarkable that the tensile steel of beam DBL30-3 had yielded when the sustaining load was applied to 90 kN. At the time of strengthening, numerous flexural cracks formed in the regions of constant moment. As the applied load was further increased, flexural cracks were not widened continuously and new diagonal cracks were formed and widened rapidly in the shear span region of beam DBL30-3 after

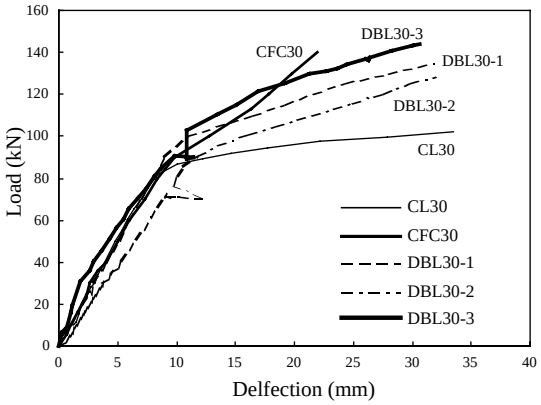

Fig. 5. Load–deflection curves for beams CL30, CFC30, DBL30-1, DBL3-2 and DBL30-3.

strengthening. Finally, shear compression failure occurred by crushing of the concrete in the shear compression zone.

Fig. 6 shows load–deflection curves of nonstrengthened control beam CL30, initially strengthened beam CFC30, and strengthened beams RDBL30-1A and RDBL30-1B, respectively. For beam RDBL30-1A, one cycles of load between 25 kN and 70 kN was applied and for beam RDBL30-1B load between 25 kN and 90 kN, after which the load was held constantly at 25 kN. It could be observed that the stiffness of RDBL30-1A, RDBL30-1B and CFC30 right follows that of CL30 before unloading. The deflection of RDBL30-1A and RDBL30-1B increased a little in the course of unloading. Load–deflection curves of RDBL30-1A and RDBL30-1B show that right after strengthening their stiffness follow that of unloading. Similar to beam DBL30-1, load–deflection curves of strengthened beam RDBL30-1A and RDBL30-1B shows no discernible differences in yielding strengths and ultimate strengths regardless of loading history.

From Figs. 5, 6 and Table 3, it was interesting to note that the strengthened beams DBL30-2 and RDBL30-1A had similar ultimate load capacities and failure modes, which suggest that rupture of CFRP laminate took place once the sustaining load reached a certain level. At that level, stress concentrations in

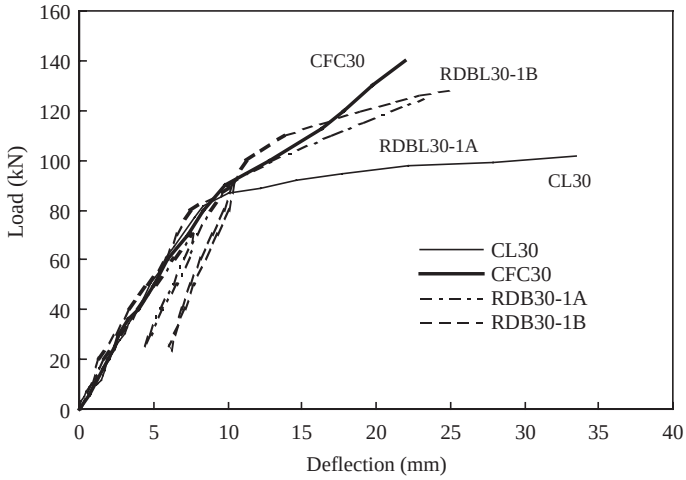

Fig. 6. Load–deflection curves for beams CL30, CFC30, RDBL30-1A and RDBL30-1B.

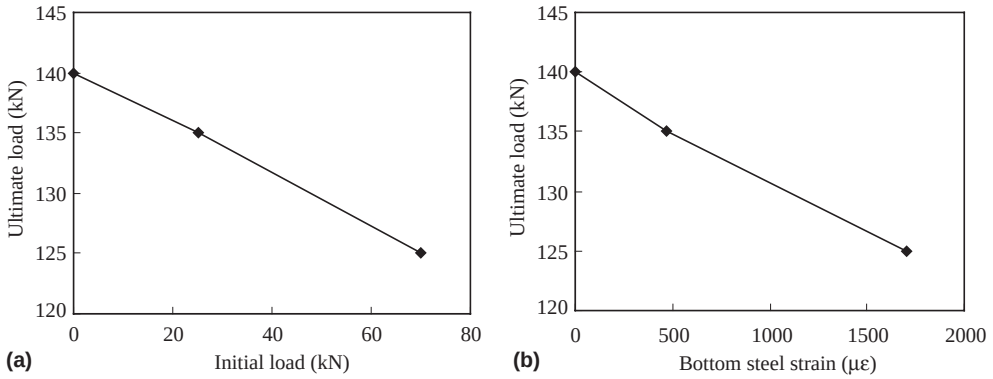

Fig. 7. Relationship of ultimate load and initial load and bottom steel strain. (a) Ultimate load–initial load curves. (b) Ultimate load–bottom steel strain curves.

CFRP laminates at the location of cracks became critical and resulted in rupture of CFRP laminates. By comparing beams DBL30-3 and RDBL30-1B, the ultimate load of strengthened beam DBL30-3 was greater than that of RDBL30-1B and different failure modes were observed. It is shown that wide diagonal cracks will result in shear compression failure while strengthening.

From Figs. 5 and 6, strengthened beams at higher levels of sustaining load have a lower ultimate strength than those of beams strengthened at lower levels of sustaining load (except for beam DBL30-3, because beam DBL30-3 failed by shear compression failure rather than flexural failure). Fig. 7(a) shows the relation of ultimate strength versus initial load for test beams CFC30, DBL30-1, and DBL30-2. It is clear from this figure that initial load is an important factor that affects the ultimate strength of RC beams strengthened with CFRP laminates at the different levels of sustaining load. It also can be seen from Table 3, if the initial load is basically same, as shown in beams RDBL30-1A and RDBL30-1B, the ultimate strength of RC beams strengthened with CFRP laminates is almost same regardless of load history at the time of strengthening.

The ductility of each beam is observed by calculating the ductility index as the ratio between the deflection of the beam at failure and its deflection at yield, as shown in Table 3. For all strengthened beams, it is clearly show that strengthening with externally bonded CFRP laminates under sustaining loads can reduce the ductility of the strengthened beams by comparison with the control beam CL30. This is consistent with the findings of Arduini and Nanni (1997) and Shahawy et al. (2001).

4.2. Relationship of loads and strains

Figs. 8–13 show the load–strain curves of CFRP, bottom steel, and top concrete for beams DBL30-1, DBL30-2, DBL30-3, RDBL30-1A, RDBL30-1B and CFC30. For beam CFC30, the steel strains and CFRP strains are essentially the same at loads below cracking of the concrete. After cracking, the strains in CFRP laminate exceeded the strains in the steel. As the load approached the yielding load for the strengthened beam, the strains in steel increased more rapidly than the strains in the CFRP. This is because the CFRP had begun to debond from the surface of concrete nearby cracks.

For beams DBL30-1, DBL30-2 and DBL30-3 with different levels of sustaining load, the initial strains of bottom steels are 472 με, 1705 με and 1973 με respectively at the time of strengthening. The load–steel strain curves of beams DBL30-1, DBL30-2 and DBL30-3 are similar to that of beam CFC30 before steel yielding, as shown in Figs. 9–11. After strengthening, the CFPR strains increased rapidly beyond yielding point. It is

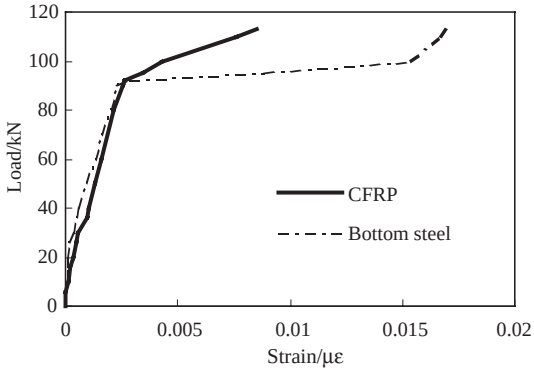

Fig. 8. Load–strain curves of CFRP and bottom steel for beam CFC30.

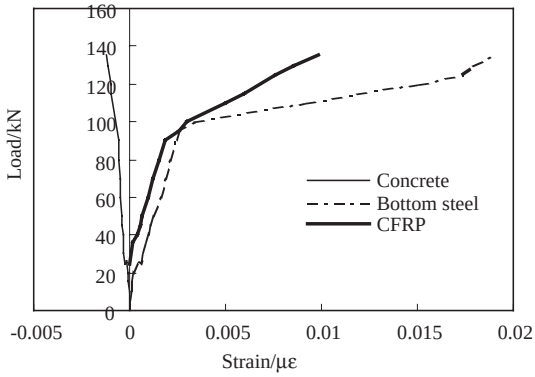

Fig. 9. Load–strain curves of CFRP, bottom steel and top concrete for beam DBL30-1.

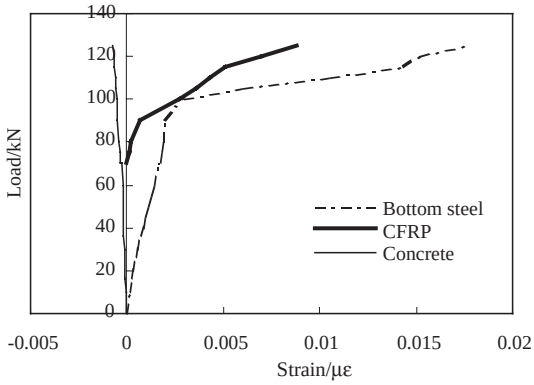

Fig. 10. Load–strain curves of CFRP, bottom steel and top concrete for beam DBL30-2.

noted that the steels strains are always greater than the CFRP strains after strengthening. This is because the initial strains in steel caused by initial loads had exited at the time of strengthening.

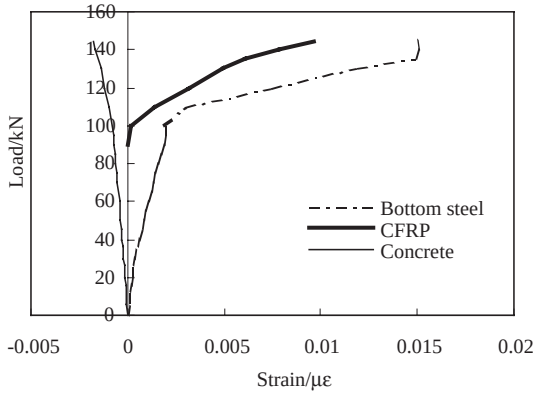

Fig. 11. Load–strain curves of CFRP, bottom steel and top concrete for beam DBL30-3.

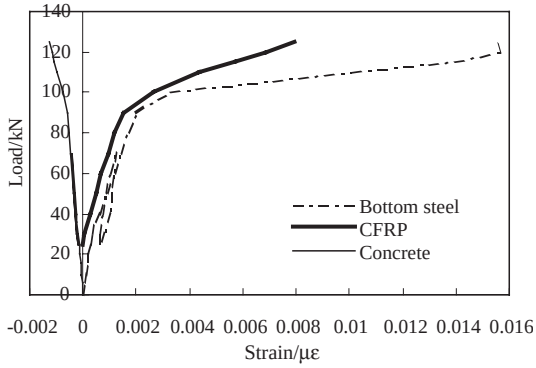

Fig. 12. Load–strain curves of CFRP, bottom steel and top concrete for beam RDBL30-1A.

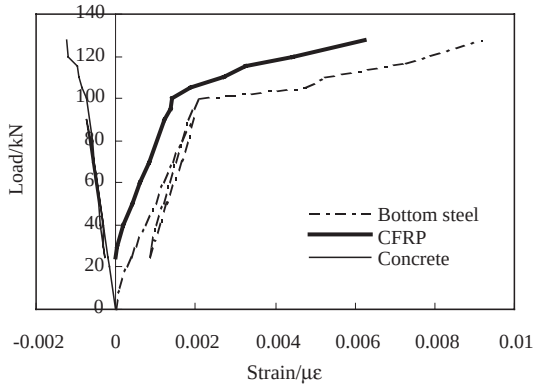

Fig. 13. Load–strain curves of CFRP, bottom steel and top concrete for beam RDBL30-1B.

For beam RDBL30-1A, one cycle of load between 25 kN and 70 kN was applied and for beam RDBL30-1B, one cycle of load between 25 kN and 90 kN, after which the load was held constant at

Table 4
Experimental and analytical results for strains

Beam designation	At initial stage					At yield stage				At ultimate stage						
	Bottom steel strain			Initial strain		Bottom steel strain	CFRP strain		Load	Bottom steel strain			CFRP strain			Load
	Experimental values	Calculated values	M[a]	Calculated values	M[a]	Experimental values	Experimental values	Calculated values		Experimental values	Calculated values	M[a]	Experimental values	Calculated values	M[a]	
CL30						2356			85	10549	16934					102
CFC30						2295	2543	2316	90	16962	10801	7866	8543	13251	9754	140
DBL30-1	472	326	548	382	692	2384	1820	1929	90	18950	10865	8051	9831	12979	9278	135
DBL30-2	1705	1482	1534	1740	1938	1932	697	559	90	17732	11237	8394	8773	12022	8435	125
DBL30-3	1913	1996	1972	2343	2492	1966	141	114	100	14995	11391	9615	7615	11601	8066	148
RDBL30-1	401	326	548	382	692	2041	1515	1929	90	15496	10865	8051	7965	12979	9278	125
RDBL30-2	281	326	548	382	692	1976	1417	1929	100	9183	10865	8051	6241	12979	9278	128

[a] M = Mahmoud's model.

25 kN for 1 week to allow for application and curing of the CFRP laminates. The load–CFRP strain curves are similar to that of beam DBL30-1and the values of steel strain are always greater than values of CFRP strain at same level of load. The steels strains increased gradually during strengthening and after 1 week the steels strains increased to 632 με for beam RDBL30-1A and to 843 με for beam RDBL30-1B.

Table 4 shows the experimental values and calculated values of steel strain and CFRP strain for all test beams. It can be observed that initial strains in steel (or initial strains in bottom face of beams) have an important effect on ultimate and yield loads, as shown in Table 4. This observation is further supported by Fig. 7(b), which shows the relationship of bottom steel strains and ultimate loads for beams CFC30, DBL30-1 and DBL30-2.

5. Theoretical model

In order to be able to predict the strength of sustaining loaded RC beams strengthened with CFRP laminates, a theoretical model has been proposed. The Hognestad stress block is used to calculate the compressive stress in concrete. The Park and Paulay numerical approximation of the Hognestad stress block is used to calculate the compressive stress in concrete. Tensile concrete is bilinear elasto-softening. Steel is elastic before yielding, and maintains a yielding stress after yielding. CFRP is perfectly linear elastic, as shown in Fig. 14. Plane cross sections remain plane during loading. The interface between adhesive and CFRP is considered stronger than the corresponding concrete–adhesive interface.

For RC beam, the member is made of two different materials, and one of them, the concrete, does not have a linear stress–strain relationship. So the initial strain at the bottom face of the RC beam is not well defined. Although the member may be prismatic, the reinforcement inside may vary from one section to another; besides, the member under service load is usually cracked transversely and diagonally; thus the moment of inertia I of the section has no meaning. Therefore, the problem is to find the means to evaluate the stiffness EI for RC member. Once the section stiffness is evaluated, the initial strain at the bottom face of the RC beam may be calculated by the usual strength of material approach. The method presented here was initiated by the Russian Academician V.I. Murashev in the early fifties with some later modifications.

Fig. 15 shows the distribution of steel stress, concrete stress and CFRP stress along member at the moment under the initial load. At the cracked section, the steel tension stress σ_s may be evaluated approximately by the following formula

$$\sigma_s = \frac{M_i}{A_s \eta h_0} \tag{1}$$

where M_i is the initial moment and ηh_0 is the moment arm at the cracked section; $\eta = 0.87$ (see reference *Code for Design of Concrete Structures GB50010-2000*).

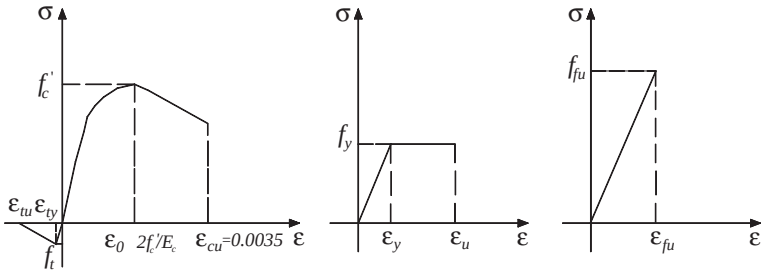

Fig. 14. Stress–strain relationships for materials, showing: (a) concrete; (b) steel; (c) CFRP.

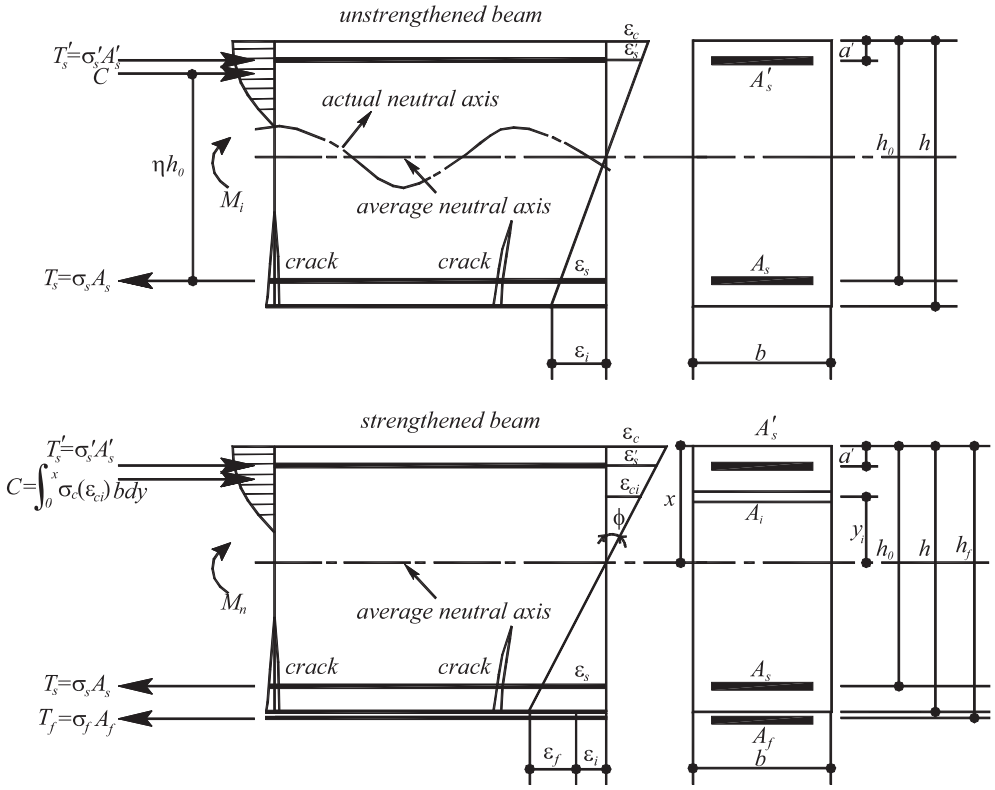

Fig. 15. Analysis discrete model.

The strain of steel ε_s at the cracked section may be expressed as

$$\varepsilon_s = \frac{M_i}{A_s \eta h_0 E_s} \tag{2}$$

The average strain of steel ε_{avg} may then be expressed as

$$\varepsilon_{avg} = \psi \frac{M_i}{A_s \eta h_0 E_s} \tag{3}$$

where ψ (see reference *Code for Design of Concrete Structures GB50010-2002*) is the coefficient to convert the steel strain at the cracked section to the average strain and

$$\psi = 1.1 - 0.65 \frac{f_{tk}}{\sigma_s \rho_{te}} \tag{4}$$

where $\rho_{te} = A_s/0.5bh$. And then the initial strain at the bottom face of RC beam under the initial load can be expressed as

$$\varepsilon_i = \frac{h}{h_0} \varepsilon_{avg} = \psi \frac{M_i h}{A_s \eta h_0^2 E_s} \tag{5}$$

From the compatibility conditions, as shown in Fig. 15, we have the expression

$$\begin{cases} \varepsilon_s = \frac{h_0 - x}{x}\varepsilon_c \\ \varepsilon'_s = \frac{x - a'}{x}\varepsilon_c \\ \varepsilon_f = \frac{h_f - x}{x}\varepsilon_c - \varepsilon_i \end{cases} \tag{6}$$

Having determined strains in concrete, steel and CFRP laminate, σ_s in tension steel, σ'_s in compression steel and σ_f in CFRP laminate are calculated using the respective stress–strain relationships for different materials, and we have the expression

$$\begin{cases} \sigma_s = E_s\varepsilon_s \\ \sigma'_s = E_s\varepsilon'_s \\ \sigma_f = E_f\varepsilon_f \end{cases} \tag{7}$$

The calculation of the concrete compression force can be performed by integrating the nonlinear concrete stress distribution over the compressed area. From the equilibrium condition, we have the expression

$$R = \int_0^x \sigma_c(\varepsilon_{ci}) b \, dy + A'_s\sigma'_s - A_s\sigma_s - A_f\sigma_f \tag{8}$$

where the symbol nomenclature is given in Appendix A.

To determine the neutral axis location x, an iterative procedure is performed by assuming a concrete strain ε_c at the extreme compression and section curvature ϕ. This procedure is continued until the value of R (Eq. (8)) is approximate zero. The nominal moment capacity for section is then calculated from the expression

$$M_n = \int_0^x \sigma_c(\varepsilon_{ci}) b(h_0 - x + y_i) dy + A'_s\sigma'_s(h_0 - a') + A_f\sigma_f(h_f - h_0) \tag{9}$$

where the symbol nomenclature is given in Appendix A.

A computer program is developed to perform the numerical analysis. The output from the program is used to calculate the ultimate loads of the test beams. The developed model is also compare with the test results obtained in this study and Mahmoud's model (see reference Mahmoud and Joseph (2000)), as shown in Table 3. Characteristic values in constitutive models for the concrete, steel reinforcing bars, and CFRP are selected from the test results. Fig. 14 illustrates those models. At the same time, a comparison between experimental values of initial strain, bottom steel strain and CFRP strain of all test beams and calculated values using predicted model and Mahmoud's model is presented, as shown in Table 4. It can be seen that the developed model is reasonably predicting those test results.

6. Conclusions

Six CFRP-laminated RC beams at the different levels of sustaining load and one control beam were tested. Three failure modes were obtained. A theoretical model to predict the strength of sustaining loaded RC beams strengthened with CFRP laminates had been proposed. Some useful conclusions are summarized as follows:

(a) Initial load is an important factor that affects the ultimate strength of RC beams strengthened with CFRP laminates at the different levels of sustaining load. Beams strengthened at higher levels of sustaining load have a lower ultimate strength than those of beams strengthened at lower levels of sustaining load.

(b) If the initial load is basically same, the ultimate strength of RC beams strengthened with CFRP laminates is almost same regardless of load history at the time of strengthening.
(c) The stiffness of strengthened beams at different levels of sustaining load basically follows that of control beam before the main steels yielding. The stiffness of strengthened beams at different levels of sustaining load is weaker than that of virgin beam strengthened with CFRP laminates and stronger than that of control beam after the main steels yielding.
(d) CFRP external reinforcement increased the load carrying capacities of load-damaged beams by 22.5–41.2%, but strengthening with externally bonded CFRP laminates under sustaining loads will reduce the ductility of the strengthened beams.
(e) A theoretical model for flexural behavior of the load-damage RC beam strengthened with CFRP laminates is also developed. The results of the method presented in this paper indicate a good agreement with experimental results.

Acknowledgements

This research was funded by the Transportation Bureau of Liaoning Province in China for the project New Crafts and New Techniques of Strengthening and Repairing Existing Bridges (NCTSREB) and was conducted in the Civil Engineering Department laboratory of Dalian University of Technology. The support of the University is gratefully acknowledged. In addition, the authors wish to thank Datong Company for their generous contribution of CFRP material.

Appendix A

a'	effective depth of compression steel
A_f	area of CFRP laminates
A_s	area of tension steel
A'_s	area of compression steel
b	width of concrete beam
E_s	modulus of elasticity of steel
E_f	modulus of elasticity of CFRP laminate
f_{tk}	standard tensile strength of concrete
h	depth of concrete beam
h_0	effective depth of tension steel
h_f	effective depth of CFRP laminate
M_i	initial moment
M_n	normal moment
R	residual cross section force
x	depth of neutral axis for cracked section
y_i	distance of segment i from neutral axis
ε_{avg}	average strain of tension steel
ε_c	strain of concrete at the edge of the compression zone
ε_{ci}	strain of segment i of the concrete compression zone or the concrete tensile zone
ε_f	strain of CFRP laminate
ε_i	initial strain
ε_s	strain of tension steel
ε'_s	strain of compression steel

η coefficient to the effective depth of tension steel
ρ_{te} steel ratio in the effective concrete tension area
σ_c stress of segment i of the concrete compression zone or the concrete tensile zone
σ_f stress of CFRP laminate
σ_s stress of tension steel
σ'_s stress of compression steel
ϕ curvature
ψ coefficient to convert the tension reinforcement strain at the cracked section to the average strain

References

Arduini, M., Nanni, A., 1997. Behavior of Precracked RC beams strengthened with carbon FRP Sheets. ASCE Journal of Composites for Construction 1 (2), 63–70.

Arduini, M., Tommaso, A.D., Nanni, A., 1997. Brittle failure in FRP plate and sheet bonded beams. ACI Structural Journal 94 (4), 363–371.

Bonacci, J.F., Maalej, M., 2000. Externally bonded fiber-reinforced polymer for rehabilitation of corrosion damaged concrete beams. ACI Structural Journal 97 (5), 703–711.

Chajes, M.J., Thomson, T.A., Januszka, T.F., Fin, W., 1994. Flexural strengthening of concrete beams using externally bonded composite materials. Construction and Building Materials 8 (3), 191–201.

Charles, W.D., 1999. FRP prestressing in the USA. Concrete International 10, 21–24.

China Ministry of Construction, 2002. Code for Design of Concrete Structures (GB50010-2002). China Architecture & Building Press, Beijing.

Erki, M.A., Rizkalla, S.H., 1993. FRP reinforcement for concrete structures. Concrete International 6, 48–53.

Jones, R., Swamy, R.N., Bloxham, J., Bouderbalah, A., 1980. Composite behavior of concrete beams with epoxy bonded external reinforcement. International Journal of Cement Composite 2 (2), 91–107.

Mahmoud, T.E.M., Joseph, W.T., 2000. Analysis of reinforced concrete beams strengthened with FRP laminates. ASCE Journal of Structural Engineering 126 (6), 684–691.

Norris, T., Saadatmanesh, H., Mohammad, R.E., 1997. Shear and flexural strengthening of R/C beams with carbon fiber sheets. ASCE Journal of Structural Engineering 123 (7), 903–911.

Saadatmanesh, H., Ehsani, M., 1991. RC beams strengthened with GFRP plates. Part I and Part II. ASCE Journal of Structural Engineering 117 (11), 3417–3455.

Sami, R., Pieere, L., 1999. Structural engineering with FRP-in Canada. Concrete International 10, 25–28.

Shahawy, M., Chaallal, O., Thomas, E.B., Adnan, E., 2001. Flexural strengthening with carbon fiber-reinforced polymer composites of preload full-scale girders. ACI Structural Journal 98 (5), 735–743.

Thomas, K., 2003. Use of Fiber Reinforced Polymer in Bridge Construction. IABSE-AIPC-IVBH Publication, Switzerland.

Yeong-soo, S., Chadon, L., 2003. Flexural behavior of reinforced concrete beams strengthened with carbon fiber-reinforced polymer laminates at different levels of sustaining load. ACI Structural Journal 100 (2), 231–240.